

First-order transition features of the 3D bimodal random-field Ising model

N G Fytas, A Malakis and K Eftaxias

Department of Physics, Section of Solid State Physics, University of Athens,
Panepistimiopolis, GR 15784 Zografos, Athens, Greece

E-mail: amalakis@phys.uoa.gr

Abstract. Two numerical strategies based on the Wang-Landau and Lee entropic sampling schemes are implemented to investigate the first-order transition features of the 3D bimodal ($\pm h$) random-field Ising model at the strong disorder regime. We consider simple cubic lattices with linear sizes in the range $L = 4 - 32$ and simulate the system for two values of the disorder strength: $h = 2$ and $h = 2.25$. The nature of the transition is elucidated by applying the Lee-Kosterlitz free-energy barrier method. Our results indicate that, despite the strong first-order-like characteristics, the transition remains continuous, in disagreement with the early mean-field theory prediction of a tricritical point at high values of the random-field.

PACS numbers: 05.50.+q, 64.60.Cn, 64.60.Fr, 75.10.Hk

Keywords: bimodal random-field Ising model, Wang-Landau sampling, free-energy barrier method

1. Introduction

The random-field Ising model (RFIM) [1, 2, 3, 4, 5, 6, 7, 8, 9, 10, 11, 12, 13, 14, 15] has been extensively studied both because of its interest as a simple frustrated system and because of its relevance to experiments [16]. The Hamiltonian describing the model is

$$\mathcal{H} = -J \sum_{\langle i,j \rangle} S_i S_j - h \sum_i h_i S_i, \quad (1)$$

where S_i are Ising spins, $J > 0$ is the nearest-neighbors ferromagnetic interaction, h is the disorder strength, also called randomness of the system, and h_i are independent quenched random-fields (RF's) obtained here from a bimodal distribution of the form

$$P(h_i) = \frac{1}{2}[\delta(h_i - 1) + \delta(h_i + 1)]. \quad (2)$$

Various RF probability distributions, such as the Gaussian, the wide bimodal distribution (with a Gaussian width), and the above bimodal distribution have been considered [17, 18, 19, 20, 21, 22, 23, 24, 25, 26, 27, 28, 29].

As it is well known, the existence of an ordered ferromagnetic phase for the RFIM, at low temperature and weak disorder, follows from the seminal discussion of Imry and Ma [1], when $D > 2$. This has provided us with a general qualitative agreement on the sketch of the phase boundary separating the ordered ferromagnetic (**F**) phase from the high-temperature paramagnetic (**P**) phase. The phase boundary (see figure 1) separates the two phases of the model and intersects the randomness axis at the critical value of the disorder strength h_c . This value of h_c is known with good accuracy for both the Gaussian and the bimodal RFIM to be 2.270(4) [26] and 2.21(1) [21, 22, 29], respectively. A most recent detailed numerical investigation of the phase boundary of the 3D bimodal RFIM appears in reference [29].

However, the general behavior of phases and phase transitions in systems with quenched randomness is still controversial [30, 31, 32], and one such lively example is the 3D RFIM, which, despite 30 years of theoretical and experimental study, is not yet well understood. In particular, the nature of its phase transition remains unsettled, although it is generally believed that the transition from the ordered to the disordered phase is continuous governed by the zero-temperature random fixed-point [7, 9, 12]. For the bimodal RFIM, the mean-field prediction [33] of a first-order region separated from a second-order region by a TCP, remains today an open controversy. This main issue has regained interest after the recent observations [34, 35] of first-order-like features at the strong disorder regime. Nowadays, this is the main conflict regarding the nature of the phase transition of the 3D bimodal RFIM, although other controversies and scenarios exist in the literature, concerning mainly the intermediate regime of the phase diagram and a possible third spin-glass phase [36, 37, 38].

Thus, the possibility of a first-order transition at the strong disorder regime has been discussed in several papers and has been supported over the years by numerical and theoretical findings. The extreme sharpness of the transition reflected in some studies in the estimated very small values of the order-parameter exponent β [19, 26] has also

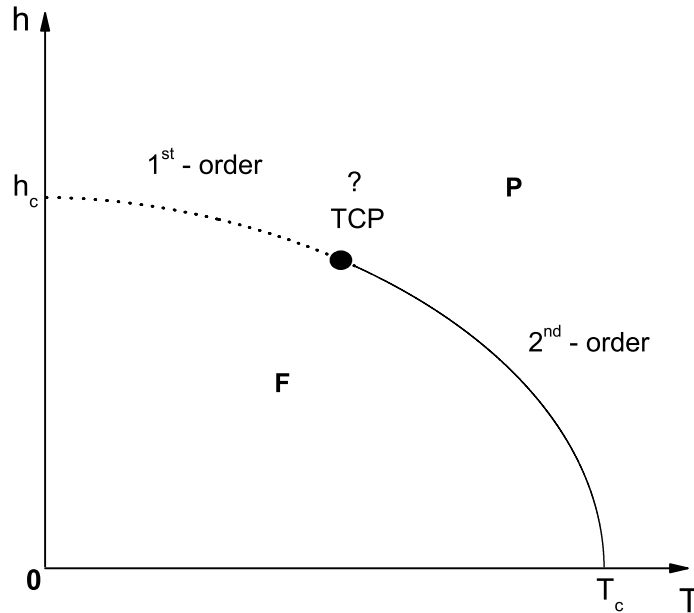


Figure 1. A sketch of the phase boundary of the 3D bimodal RFIM, where h_c is the critical disorder strength and T_c the critical temperature of the pure 3D Ising model. The question-mark refers to the mean-field prediction of a tricritical point (TCP), where the transition supposedly changes from second-order at low-fields (solid line) to first-order at high-fields (dotted line).

been reinforcing such first-order scenarios. In particular first-order-like features, such as the appearance of the characteristic double-peak (dp) structure of the canonical energy probability density function (PDF), have been recently reported for both the Gaussian and the bimodal distributions of the 3D RFIM. Particularly, Wu and Machta [28], using the Wang-Landau (WL) approach [39, 40, 41], reported such properties for the Gaussian RFIM at a strong disorder strength value $h = 2$ below their critical randomness ($h_c = 2.282$). Moreover, Hernández and Diep [34] have emphasized that they have found evidence for the existence of a TCP in the phase diagram of the bimodal RFIM, in agreement with the early predictions of mean-field theory [33]. These authors have also observed, at the disorder strength value $h = 2.1$, using standard and histogram Monte Carlo methods [34] and more recently the WL algorithm [35], the same first-order-like characteristic dp structure and concluded that there is a TCP at some intermediate value of the disorder strength.

The existence of a dp structure in the canonical PDF is related to a convex dip in the microcanonical entropy and it is known that for some systems a mere observation of this structure is not sufficient for the identification of a first-order transition. The Baxter-Wu [42, 43, 44] and four-state Potts models in 2D [45] are well-known examples of such systems undergoing, in the thermodynamic limit, second-order phase transitions. Recently, Behringer and Pleimling [46] have demonstrated for these two models that,

the appearance of a convex dip in the microcanonical entropy can be traced back to a finite-size effect different from what is expected in a genuine first-order transition. In other words, the pseudosignatures of a first-order transition are finite-size effects, which can be understood within a scaling theory of continuous phase transitions and such first-order-like features cease to exist in the thermodynamic limit. Similar first-order-like properties have been observed in many other finite systems, such as the well-known examples of the fixed-magnetization versions of the Ising model, where it has been also shown that these finite-size effects disappear in the thermodynamic limit [47, 48, 49].

The present paper, is the first extensive numerical investigation of this fundamental issue for the 3D bimodal RFIM. We proceed, having in mind that a mere observation of a first-order structure is not sufficient for the identification of the transition. This is especially true for the present model, since its critical behavior is obscured by strong and complex finite-size effects, involving also the important issue of the lack of self-averaging [28, 50, 51, 52, 53, 54]. Thus, for a clear identification of the order of the transition, we implement an appropriate version of the Lee-Kosterlitz (LK) free-energy barrier method [55]. Initially, we used a straightforward one-range (one-R) WL sampling on a set of a small number of RF realizations, at two values of the disorder strength, $h = 2$ and $h = 2.25$. This attempt enabled us to observe the behavior of the free-energy barrier and the latent heat and indicated that the transition remains continuous at the strong disorder regime. By a second substantial attempt, using a combined more efficient numerical scheme, we simulated large numbers of RF realizations and verified that, indeed, the first-order-like transition signatures are finite-size effects that disappear in the thermodynamic limit.

The remainder of the paper is as follows: subsection 2.1 gives a summary of the WL and Lee methods. In particular, we explain, discuss, and give details of two different numerical strategies, called hereafter as one-R approach and high-level one-R approach. We continue, in subsection 2.2, to present the application of the LK free-energy barrier method [55] on the numerical data, obtained via a straightforward application of the one-R WL implementation on a small ensemble of RF realizations for two values of the disorder strength, $h = 2$ and $h = 2.25$. The same method is applied in subsection 2.3 on the numerical data obtained via a new proposal capable to simulate large numbers of RF realizations, at the disorder strength value $h = 2$. As will be explained in subsection 2.1, this latter strategy is an efficient and accurate WL approach, which combines in three stages, the multi-range (multi-R) WL algorithm, the high-level one-R WL approach, and a final quite long Lee run, to obtain an alternative, and presumably most accurate, density of states (DOS). Subtle points behind the necessity of implementing such an elaborate scheme will be discussed appropriately in the sequel. Finally, we summarize our conclusions in section 3.

2. Numerical schemes. Identification of the order of the transition

2.1. Sampling the RFIM by the WL and Lee methods

Several sophisticated simulation techniques, such as cluster algorithms and flat-histogram approaches, have been used to study the RFIM [11, 24, 34, 35, 56, 57, 58, 59], while graph theoretical algorithms have been used to study properties of the ground-states of this model [14, 20, 21, 22, 23, 25, 26, 28, 60]. Entropic sampling methods such as the Lee [61, 62] and WL [39, 40, 41] methods are efficient alternatives for complex systems and systems that undergo first-order transitions. Accordingly, we will implement a combination of such numerical approaches, based mainly on the WL method, to study the nature of phase transition of the 3D bimodal RFIM at the strong disorder regime. The WL algorithm is one of the most refreshing improvements in Monte Carlo simulation and has been applied to a broad spectrum of interesting problems in statistical mechanics and biophysics [62, 63, 64, 65, 66, 67, 68, 69, 70, 71, 72, 73].

To apply the WL algorithm, an appropriate energy range of interest has to be identified. A WL random walk (single spin flip) is performed in this energy subspace. Trials from a spin state with energy E_i to a spin state with energy E_f are accepted according to the transition probability

$$p(E_i \rightarrow E_f) = \min \left[\frac{G(E_i)}{G(E_f)}, 1 \right]. \quad (3)$$

During the WL process the DOS $G(E)$ is modified ($G(E) \rightarrow f * G(E)$) after each spin flip trial by a modification factor $f > 1$. The WL iterative process ($j = 1, 2, \dots$) is defined as a process in which successive refinements of the DOS are achieved by monotonically decreasing the modification factor f_j . Most implementations use an initial modification factor $f_{j=1} = e \approx 2.71828\dots$ and a rule $f_{j+1} = \sqrt{f_j}$, while a 5% – 10% flatness criterion (on the energy histogram) is applied in order to move to the next refinement level ($j \rightarrow j + 1$) [39, 40]. The WL process is terminated in a sufficiently high-level, at which $f \approx 1$ (typically $f = 1.000\ 00001$). Note that the detailed balanced condition is satisfied in the limit $f \rightarrow 1$. There have been several papers in recent years dealing with improvements and sophisticated implementations of the WL iterative process [62, 63, 64, 65, 66, 67, 68, 69, 70, 71, 72, 73]. Some of these suggestions appeared in studies of efficiency and convergence of the WL iterative process [62, 64, 66, 68, 71], while others were proposed in applications of the WL scheme in simulating several models of statistical mechanics [63, 65, 67, 69, 70, 72, 73]. In our recent study, of the first-order transition of the triangular SAF model [73], we also used a final stage of an unmodified ($f = 1$) Lee entropic simulation [61] by applying after, a relatively long run, a Lee correction to an already good approximation obtained by the WL process. This final Lee entropic stage will be also followed here and it is hoped that through this practice we improve accuracy, but also obtain an idea of the level of approximation, since starting with a very accurate DOS and using a sufficiently long run, the Lee correction should produce an almost identical DOS.

In our implementation of this Lee entropic stage, we start with a very good approximation of the DOS [$G_{WL}(E)$], obtained by the WL process after a large number n of WL iterations (we choose $n = 20$) in which we follow the above described reduction of the modification factor f ($f_{j=1} = e \approx 2.71828 \dots$, $f_{j+1} = \sqrt{f_j}$, $j = 1, 2, \dots, n$). This good estimate of the DOS is used to determine the transition probabilities [equation (3)] for an unmodified ($f = 1$) random walk in energy space, as described by Lee [61], in a process which obeys now the detailed balance condition (equation (5) of reference [61]) and produces an almost flat energy histogram $H(E)$ in the long run. Note that, a completely flat histogram (besides statistical fluctuations) will be produced in case one is using the exact DOS, as pointed out by Lee [61]. However, provided that the Monte Carlo time is long compared to the ergodicity time, we obtain a better estimate for the DOS, i.e. $G_{Lee}(E)$, by the following prescription:

$$\log G_{Lee}(E) = \log G_{WL}(E) + \log H(E). \quad (4)$$

The implementation described above is in fact very similar to the suggestion of reference [62] for a repeated application of the above Lee correction scheme, after a first stage of the WL process consisting of n WL iterations. Then, the successive Lee corrections obtained by repeated applications of our equation equation (4) (equation (15) of reference [62]) will improve the original DOS, as shown in reference [62]. This repeated application was started in [62] at an early WL iteration level ($n = 14$) and was tested favorably compared to the simple WL process.

The multi-R WL approach is the implementation of the method in which one splits the energy range in many subintervals [39]. This is almost a necessity for very large lattices and the subintervals used are slightly overlapping. The DOS's of the separate pieces are joined at the end of the process. This multi-R approach is, of course, a much faster process compared with a straightforward one-R implementation and in many cases has provided very accurate results for very large systems [39]. Although, several papers have pointed out problems with the accuracy, efficiency and convergence of the WL method [62, 64, 66, 71], several important related questions are still unanswered, or at least, not well understood. Possible distortions (systematic errors) induced on the DOS by using a multi-R WL approach have not been adequately discussed in the literature. Of course, boundary effects of WL sampling in restricted energy subspaces (multi-R processes) were observed, analyzed and successfully resolved in reference [41]. However, subtle effects, coming from the inevitable breaking of the ergodicity of phase space, may be inherent in any restricted energy subspace or multi-R method. Below, we will present a novel case coming from our recent studies of the RFIM. An escape from this novel, rather discouraging case, will be proposed by compromising between the multi-R and the one-R approach.

The WL method has been already applied to the RFIM in several previous studies. Two such recent investigations, directly related to this work, have been presented for the Gaussian [28] and the bimodal RFIM [35]. As pointed out in the introduction, both of these studies have observed and discussed first-order-like properties of the RFIM at

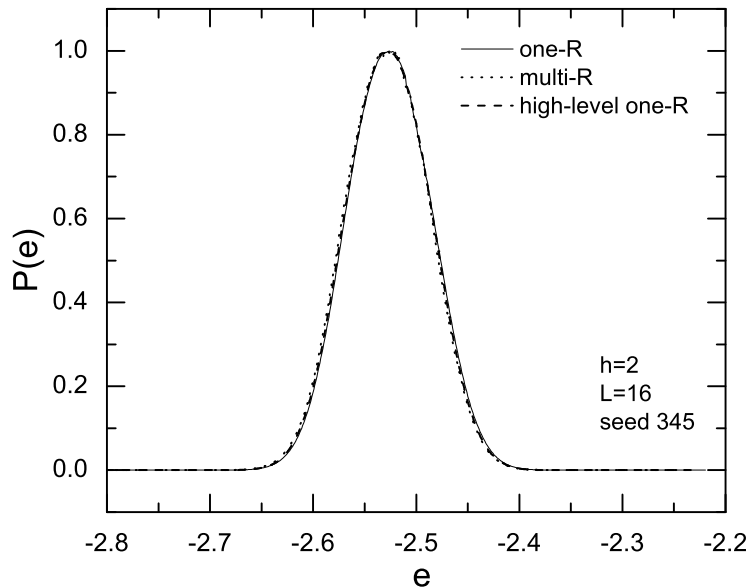


Figure 2. A typical sp energy PDF for a RF realization at the temperature corresponding to the specific heat peak. Three almost coinciding energy PDF's are shown, corresponding to the three approaches discussed in the text, i.e. one-R, multi-R, and high-level one-R. The PDF's are expressed as a function of the energy per site $e(= E/N)$.

the strong disorder regime. The WL method was also implemented, in restricted energy subspaces, for the study of the bimodal RFIM in our earlier studies [54]. In these papers, a systematic restriction of the energy space, with increasing the lattice size, was used and explained in detail in order to further improve the efficiency of the WL method. This approach followed the general spirit of our earlier proposal of estimating the critical behavior of classical statistical systems via entropic simulation in dominant energy subspaces. This restrictive version, utilizes the so called critical minimum energy subspace (CrMES) technique [72] to locate and study finite-size anomalies of systems by carrying out the random walk only in the dominant energy subspaces. Generally, our finite-size scaling studies have shown that this restrictive practice can be followed in systems undergoing second-order [72] and also first-order transitions [73]. Furthermore, in our recent study of the phase diagram of the 3D bimodal RFIM [29] we have used a one-R and looser version of this restrictive scheme. In this case we have used the high-levels of the one-parametric WL method as a convenient entropic vehicle, by which the accumulation of the two-parametric, exchange-energy, field-energy, histograms would provide, via extrapolation, a good approximation for the two-parameter DOS necessary to find several points of the phase diagram. Since substantial histogram accumulation is necessary to overcome statistical errors in such an application, the faster multi-R approach was not used and for having a reliable extrapolation scheme the energy

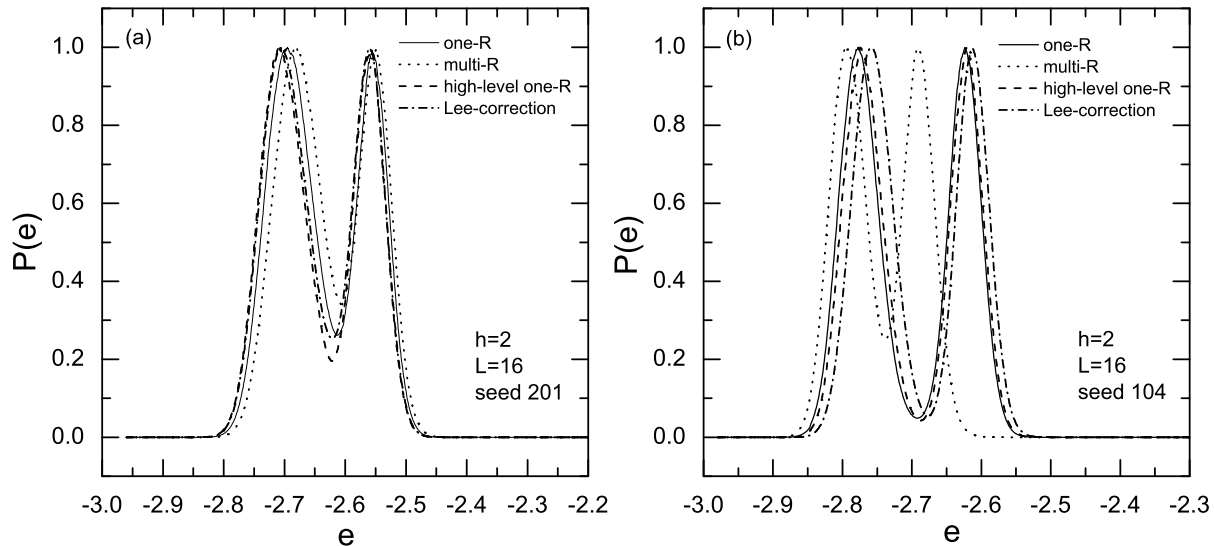


Figure 3. Different energy PDF's for two RF realizations estimated by the numerical approaches discussed in the text: one-R, multi-R, high-level one-R, and final Lee. The PDF's are determined at the temperature where the two peaks are of equal height. Note that, only the RF realization of panel (b) shows a large distortion of the dp structure in the case of the multi-R approach, when compared to the other (one-R) schemes.

spectrum for the simulation was restricted only from the high-energy side, while the entire low-energy part of the spectrum down to the ground-state was included. For the restriction of the high-energy side we used our data from our previous study of the model at the value $h = 2$. However, for the larger lattice sizes, one can conveniently avoid the ground-state neighborhood.

In the present study, we initially used the data of this last straightforward one-R approach [29] to observe the behavior of the dp structure of some typical RF realizations at the strong disorder regime ($h = 2$ and $h = 2.25$). As already pointed out, these results appear in subsection 2.2 and are obtained by using a final of $j = 20$ WL iteration levels for the smaller lattices up to $L = 16$ and a final of $j = 24$ WL iteration levels for the larger sizes ($L \geq 20$).

Subsequently, and in order to simulate larger numbers of dp RF realizations, we decided to test carefully and then use a multi-R approach. Thus, we compared the (energy PDF) dp's of some typical RF realizations obtained by the one-R approach with the dp's obtained by a usual multi-R approach (corresponding to the same or an even higher level of the WL process). For some RF realizations the energy PDF graphs almost coincided and this was especially true for the single-peak (sp) RF realizations. But also for several dp RF realizations the corresponding graphs were close enough and within statistical errors. Figures 2 and 3(a) show two such examples, one corresponding to a sp RF realization and one to a dp RF realization. However, for some peculiar dp

RF realizations the dp graphs resulting from the multi-R approach were dislocated and with a rather large deviation in their depth, when compared with the dp energy PDF graphs obtained for the same RF realizations by the one-R approach. Figure 3(b) shows a characteristic case, corresponding to a serious dislocation and underestimation of the dp structure. Furthermore, it was observed that the dp details were very sensitive to the division of the energy range to subintervals, indicating that the distortion errors were due to the application of the multi-R approach. After several tests, we concluded that this peculiar problem is related to the division of the dp range in subintervals. It appears that for some RF realizations, the structure of the convex dip in the microcanonical entropy is not well estimated by using the multi-R approach within the dp range. We concluded that the details of the convex dip are sensitive to possible subtle violations of ergodicity, induced by the multi-R approach. Thus, we tried to find an alternative that will not suffer from this problem and still be efficient enough so that we could simulate large numbers of RF realizations. The developed method will be called high-level one-R WL approach and is a further sophistication in the same spirit of our earlier practice in optimizing the WL entropic sampling. It combines the multi-R and the one-R approaches in an almost optimum way and seems to meet the needs of a careful estimation of the dp structure of the present model.

The details of this approach, applied here only for $h = 2$, are as follows. For each lattice size, a wide energy subspace restricted mainly from the high-energy side is divided in relatively small subintervals, of the order of 100 energy levels and a multi-R approach is applied up to the $j = 16$ WL iteration level. This completes the first stage of the approach and the DOS obtained is used to estimate for each particular RF realization the dp range. This identification is easily achieved by using our earlier practice for first-order transitions [73], by finding the appropriate temperature of equal height for the two peaks of the energy PDF. The energy PDF at this temperature is normalized so that the height of the two peaks is unity and corresponds to energies E_1 and E_2 . The dp range is now identified as follows: the left-end of the dp subspace is the energy E_{1-} , for which the density becomes greater than 10^{-6} starting from E_{min} and respectively the right-end of the dp subspace is the energy E_{2+} , for which also the density becomes greater than 10^{-6} starting from E_{max} . Having this first approximate identification of the dp subspace, a one-R WL walk is again performed at the level $j = 16$ in a subspace which is wider than the dp subspace by a factor of 10% at each end. In other words, the left-end E_{1-} is shifted to the left by 10% of the dp range and correspondingly the right-end E_{2+} is shifted to the right by the same amount. After the $j = 16$ one-R approach the ends of the dp subspace are re-estimated and fixed. The one-R WL approach is then carried on only in this dp subspace for the higher levels $j = 17, 18, 19$, and $j = 20$. This completes the second stage of our approach. Finally, an unmodified Lee random walk is performed in this dp subspace, using the last approximation of the WL DOS for the transition rates. The Lee correction is applied at the end to produce an alternative estimate for the DOS. The time duration of this last Lee run is taken to be equal to the duration of the four last one-R WL iterations. For some RF realizations, this one-R

process was pushed up to $j = 24$ to observe differences and estimate statistical errors. In all cases, these statistical errors were very small, much smaller than the observed sample-to-sample fluctuations (see also discussion in subsection 2.3 below).

We give here some details for the sizes of the dp subspaces involved in the above scheme. For $L = 24$, the initial restricted energy subspace used for the multi-R process was of the order of 2600 energy levels, i.e. counting energy levels from the all minus spin state this was the subspace defined by the levels $ie = 100$ to $ie = 2700$. Typically the size of the resulting dp subspace was of the order of 800 energy levels, which is about 30% of the initial restricted energy subspace. The left-end E_{1-} roughly fluctuated, for a sample of 100 RF realizations, between the levels $ie = 600 - 900$, while the right-end E_{2+} between the levels $ie = 1400 - 1700$. Respectively, for $L = 32$ the initial restricted energy subspace used for the multi-R process was of the order of 4200 energy levels, defined by the levels $ie = 300$ to $ie = 4500$. Typically, the size of the resulting dp subspace was again of the order of 800 energy levels, which is about 20% of the initial restricted energy subspace. In this case, E_{1-} fluctuated, again for a sample of 100 RF realizations, between the levels $ie = 1450 - 1950$, while E_{2+} between the levels $ie = 2250 - 2750$.

To conclude the above remarks, let us point out that, for a typical RF realization, when $L = 24$, a safe dp location is established after the $j = 16$ one-R level and consists of about 960 energy levels ($800 + 20\% \times 800$). It is quite astonishing that the same energy space requirements are needed also for $L = 32$ and this is related to the final conclusion of this paper, that the dp peak width, in units of energy per site, tends to zero in the limit $L \rightarrow \infty$. The above remarks clarify also the reasons behind the efficiency of the present proposal (high-level one-R approach). Typically, for one RF realization of a lattice size $L = 16$ at the disorder strength value $h = 2$ (figure 3), the simulation time t for the one-R WL process, in all the energy subspace (E_{min}, E_{max}), was of the order of 12 hours performed in a Pentium IV 3GHz. The simulation times corresponding to the other cases presented in panel (b) of figure 3 are as follows: multi-R approach $t/24$ and high-level one-R WL approach together with the final Lee run $t/9$. We may also point out, that very recently, Fernández *et al* [74], have found that the phase space for the first-order transition of the 3D site-diluted four-states Potts model is reduced, as compared with the expectations from simulations in small lattice sizes, a behavior very similar to the above observations. Their microcanonical approach [74, 75] may also be an interesting alternative, not used previously, for the study of the present model.

2.2. One-R WL approach. Transition-identification by the LK method

In this subsection, we present the application of the LK method on the numerical data obtained by the one-R WL method. As mentioned in the previous subsection, the one-R approach on both values of the disorder strength ($h = 2$ and $h = 2.25$) was applied in a wide energy spectrum and we have conveniently avoided a suitable ground-state neighborhood. The total number of RF realizations simulated (N_{tot}) varies from 20 realizations for $L \leq 24$ to 10 realizations for $L > 24$.

From a traditional point of view, the nature of a phase transition can be, in principle, determined by examining the finite-size scaling of various thermodynamic quantities, such as the specific heat and susceptibility peaks. These two quantities, as well as others, are expected, from the general theory of first-order transition, to follow an L^d divergence and may be used as indicators of the order of the transition. However, this practice is very often inconclusive even for simple systems and may be seriously questioned for random systems in which fundamental and subtle problems exist concerning the averaging process over disorder. For the present RFIM, the lack of self-averaging observed by the present authors [54] (see also references [28, 50, 53]), may be of crucial importance especially in trying to construct convenient indicators for the nature of the transition at the strong disorder regime. First-order-like realizations are expected to exhibit sharp specific heat and susceptibility peaks, such as that observed also in the Gaussian case studied by Wu and Machta [28]. Therefore, according to our previous papers [54] and as pointed out also in reference [35] the information concerning an individual first-order-like realization will be washed out - as a result of the strong fluctuation in the pseudocritical temperature - in considering for instance the behavior of the average specific heat curve.

From the above discussion, it is obvious that in order to avoid problems with the lack of self-averaging property, the first-order-like features of each realization must be computed separately and the disorder average should be applied at the end in the proper first-order indicator. The most convenient approach in this case is to use the free-energy barrier method proposed by Lee and Kosterlitz [55]. This method has been already successfully applied by Chen *et al* [76] for the study of an analogous disordered system, namely the two-dimensional eight-state Potts model with quenched bond randomness. Thus, we will proceed now to apply the LK method for the identification of the transition of the bimodal RFIM at the strong disorder regime. The method is well-known and has been widely applied to several spin models [55, 73, 76], so we will proceed giving only the necessary definitions adapted to the present disordered system.

Figure 4(a) illustrates, in the main frame, the typical dp energy probability distribution (seed 1447) and in the inset the corresponding sharp specific heat peak of a first-order-like realization on a cubic lattice of linear lattice size $L = 16$ at the disorder value $h = 2.25$. With the help of this figure, let us define the surface tension $\Sigma(L) = \Delta F(L)/L^{d-1} (= \Delta F(L)/L^2)$ for each dp realization, where the definition of the LK free-energy barrier is, using the canonical energy PDF $P(e)$, $\Delta F = k_B T \ln [P_{max}/P_{min}]$ ($e = E/N$, as in figure 2). Therefore, with the help of only the generated dp realizations (N_{dp} is their number, see also the discussion below), we define the disorder average of the surface tension, which is proposed as the relevant indicator representing the ensemble of dp realizations, as

$$[\Sigma(L)]_{av} = \frac{1}{N_{dp}} \sum_{i=1}^{N_{dp}} \Sigma_i(L). \quad (5)$$

The second important ingredient in the size development of the observed first-order-like

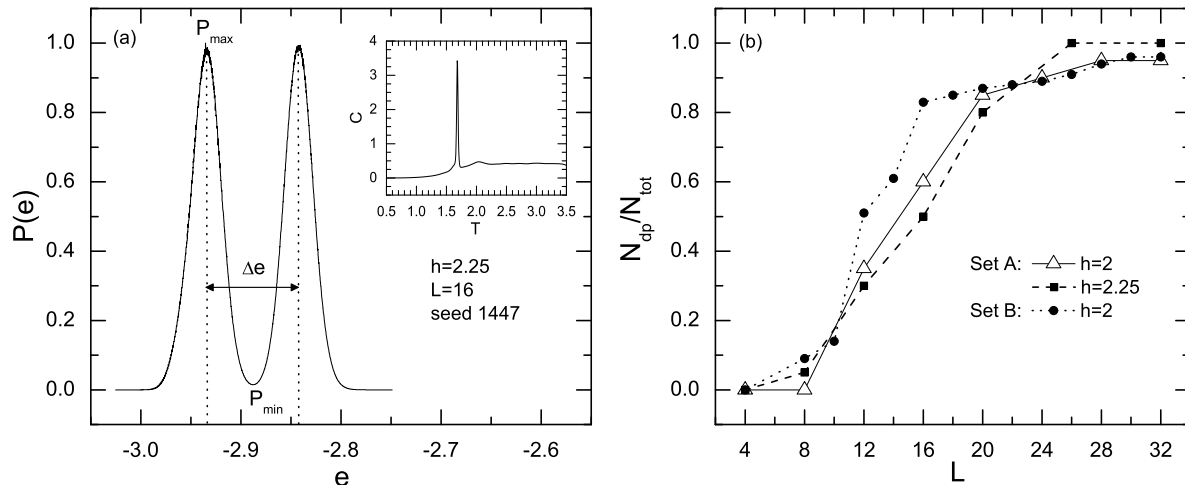


Figure 4. (a) Energy PDF at the temperature where the two peaks are of equal height for a first-order-like RF realization of a lattice size $L = 16$ at disorder strength $h = 2.25$. The inset shows the corresponding sharp specific heat peak. (b) Ratio N_{dp}/N_{tot} of realizations showing a dp energy PDF in an ensemble of N_{tot} number of realizations as a function of the linear system size L . Set A: $\{h = 2; L = 4, 8, 12, 16, 20, 24, 28, 32\}$ (open triangles) and $\{h = 2.25; L = 4, 8, 12, 16, 20, 26, 32\}$ (filled squares). Set B: $\{h = 2; L = 4, 8, 10, 12, 14, 16, 18, 20, 22, 24, 26, 28, 30, 32\}$ (filled circles).

properties of the 3D bimodal RFIM is the behavior of the width $\Delta e(L)$ of the individual dp's, representing the latent heat of the transition, in the case of a first-order transition. Again with the help of the illustration in figure 4(a), we define the disorder average over the ensemble of dp realizations of the width of the transition as

$$[\Delta e(L)]_{av} = \frac{1}{N_{dp}} \sum_{i=1}^{N_{dp}} \Delta e_i(L). \quad (6)$$

Figure 4(b) presents the relative number of such first-order-like realizations N_{dp} , in a total number of N_{tot} realizations. Set A refers to the straightforward one-R WL approach for the two values $h = 2$ and $h = 2.25$ of the disorder strength. The observed increase with lattice size of the probability for such first-order-like realizations, is in qualitative agreement with the general behavior reported by Wu and Machta [28] for the Gaussian RFIM. From Table V of reference [28] one observes a general tendency of the ratio N_{dp}/N_{tot} to increase with the system size and the disorder strength and since we are studying the system at a relatively higher disorder strength value, our ratios are quite comparable with those given in Table V of reference [28], although the latter refer to the Gaussian RFIM. Clearly, at the strong disorder regime and as the lattice size increases, the percentage of realizations showing a dp in the energy probability distribution increases and approaches unity very rapidly. Thus, in our case for lattice sizes of the order of $L \geq 24$ almost all of the simulated realizations showed a dp energy probability distribution (in fact for the value $h = 2.25$ the ratio N_{dp}/N_{tot} reached unity).

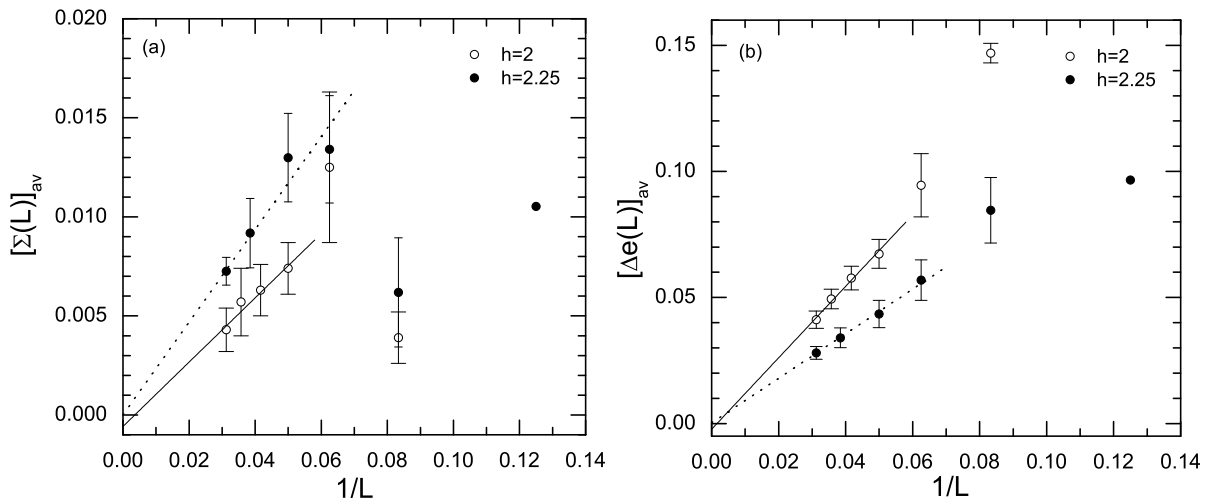


Figure 5. $1/L$ -behavior of $[\Sigma(L)]_{av}$ (a) and $[\Delta e(L)]_{av}$ (b) at $h = 2$ (open circles) and $h = 2.25$ (filled circles) for $L \geq 8$. Sample-to-sample fluctuations are illustrated by the error bars. The solid and dotted lines are corresponding linear fits for the larger sizes ($L \geq 16$). In both panels and for both values of the disorder strength, a limiting value very close to zero for the free-energy barrier and the latent heat is obtained, indicating a continuous transition.

This observation explains why we have used only the N_{dp} realizations in the disorder averaging (equations (5) and (6)), since it implies that only these realizations are of interest, since for large lattices these will dominate the behavior. This practice avoids transient effects, coming from the small lattices, and we have further pushed it by applying here a quite rather strict criterion for the definition of the dp realizations: $P_{min} < 0.75$ (note the normalization of the energy PDF: $P_{max} = 1$ in figure 4(a)).

The behavior of the disorder average of the surface tension $[\Sigma(L)]_{av}$, for both $h = 2$ and $h = 2.25$, as a function of the inverse lattice size, is shown in figure 5(a). Linear fits are applied only for the data corresponding to sizes $L \geq 16$. From these linear plots (solid and dotted lines) it appears that $[\Sigma(L)]_{av}$ approaches zero, as expected at a second-order transition. This observation strongly indicates that, what we are observing from these dp realizations for small sizes is a finite-size effect that will disappear in the thermodynamic limit. The solid and dotted lines explicitly illustrate this, using a linear extrapolation of the large size data for $h = 2$ and 2.25, giving an almost zero surface tension in the limit $L \rightarrow \infty$ for both values of the disorder strength: 0.0006 ± 0.009 and 0.000009 ± 0.03 , respectively. Furthermore, figure 5(b) depicts an undeniable steady approach to zero of the above representative width, again for both values of the disorder strength $h = 2$ and $h = 2.25$. The linear extrapolation attempts are shown by the solid and dotted lines and give also an almost zero value for the latent heat of the order of -0.002 ± 0.004 and 0.0002 ± 0.008 , respectively. This is a further strong manifestation in favor of the continuous phase transition scenario. Thus, the evidence presented in this subsection for the 3D bimodal RFIM are in agreement with the favored view of most

existing theoretical and numerical studies [17, 19, 54, 57] that the phase transition of the 3D RFIM is of second-order. In order to present even stronger numerical evidence of a vanishing (in the limit $L \rightarrow \infty$) surface tension we will now attempt to go well beyond the observation of several typical RF realizations. In the next subsection, numerical evidence will be presented for the finite-size behavior of the free-energy barrier and the latent heat of much larger ensembles of RF realizations, obtained via the efficient high-level one-R entropic scheme described in subsection 2.1.

2.3. Revisiting the order of the transition by the high-level one-R WL approach

In this subsection, we will apply the LK method on the numerical data obtained by our second numerical strategy, described in subsection 2.1. Using the high-level one-R WL approach and its final Lee correction, we generated numerical data for large number of RF realizations at the disorder strength value $h = 2$. In this case, the number N_{tot} of realizations varied so that for every lattice size $L > 10$, 100 RF realizations showing a dp structure in the energy PDF ($N_{dp} = 100$) were simulated. For the small sizes $L = 8$ and $L = 10$ only 10 dp realizations have been identified in respective ensembles of $N_{tot} = 112$ and $N_{tot} = 74$ simulated realizations.

Set B in figure 4(b) refers to the above mentioned large ensembles of realizations simulated at $h = 2$. In the present case, a looser criterion ($P_{min} < 0.9$) was applied for the identification of a dp realization. The corresponding ratios N_{dp}/N_{tot} in figure 4(b) almost coincide for set A and set B, for the larger sizes. This is easily explained by observing that for large sizes almost all dp realizations appear to have a quite deep minimum in the energy PDF. However, as it will be shown below, the scaling of these minima will not support a first-order character of the transition.

Figure 6 presents our results for the disorder averaged surface tension $[\Sigma(L)]_{av}$ and latent heat $[\Delta e(L)]_{av}$ over set B of realizations at $h = 2$. The open triangles refer to the results obtained by the high-level one-R WL approach, whereas the filled circles to those estimated from the final Lee correction. In panel (a) the values of $[\Sigma(L)]_{av}$ are shown for $L \geq 8$. Although for sizes up to $L = 18$ $[\Sigma(L)]_{av}$ seems to steadily increase, for sizes $L \geq 20$ a clear approach to zero is observed and this fact is compatible to the behavior of figure 5(a). Respectively, panel (b) shows the values of $[\Delta e(L)]_{av}$, also for $L \geq 8$. The final large size decrease, is explicitly illustrated by the solid line (in both panels of figure 6), revealing the true asymptotic behavior of these quantities. Specifically, the solid lines are linear fits performed on the data obtained by the high-level one-R WL approach, for the larger lattice sizes studied ($L \geq 16$), giving: -0.00171 ± 0.0009 and -0.00852 ± 0.005 for $[\Sigma(L \rightarrow \infty)]_{av}$ and $[\Delta e(L \rightarrow \infty)]_{av}$, respectively. As it can be seen from this figure, the data obtained by the Lee correction process would practically provide the same limiting values for the surface tension and the latent heat and therefore the corresponding linear fits are not shown. Noteworthy that, a comparison between statistical errors and sample-to-sample fluctuations is quite apparent in this figure. The values of $[\Sigma(L)]_{av}$ and $[\Delta e(L)]_{av}$ estimated over the two sets of realizations (set A and

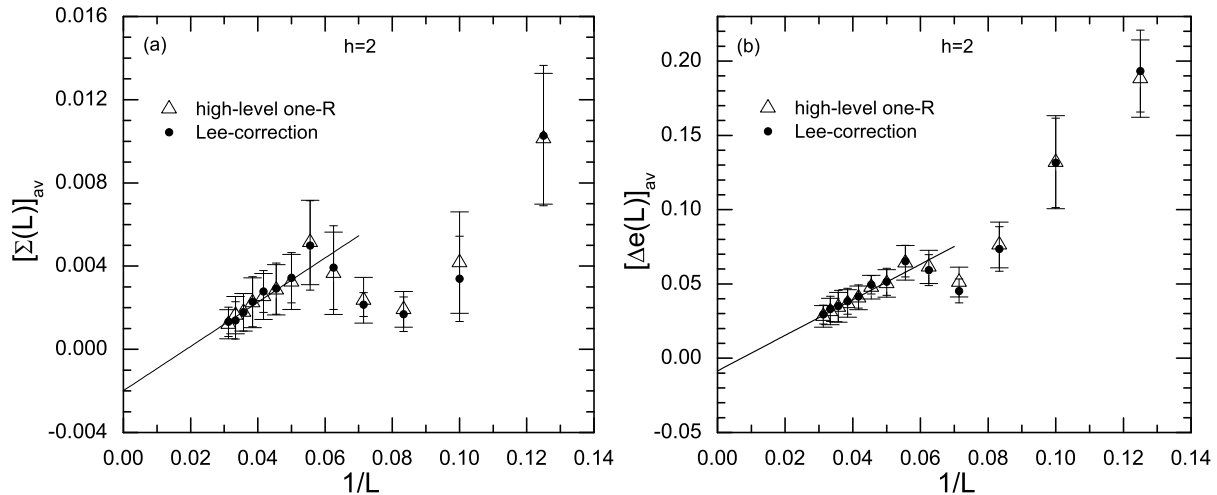


Figure 6. $1/L$ -behavior of $[\Sigma(L)]_{av}$ (a) and $[\Delta e(L)]_{av}$ (b) at $h = 2$ and for $L \geq 8$. Two set of results are shown, corresponding to the high-level one-R WL approach (open triangles) and the Lee correction (filled circles). The sample-to-sample fluctuations for the case of the high-level one-R WL results are shown with the larger cap width. The solid lines are the corresponding linear fits for $L \geq 16$, giving very small, close to zero, negative values for $[\Sigma(L \rightarrow \infty)]_{av}$ and $[\Delta e(L \rightarrow \infty)]_{av}$, thus verifying the scenario of figure 5.

set B) for $h = 2$ estimated via the two different numerical strategies presented in this paper are of the same order. Those of set A are slightly larger as a consequence of the more strict criterion, $P_{min} < 0.75$, used for the identification of the dp RF realizations.

The interesting first-order-like properties of the model, reported by Hernández and Diep [34] and Hernández and Ceva [35] for the bimodal RFIM and by Wu and Machta [28] for the Gaussian RFIM, have added more complication and novelty to the RFIM. The first-order-like characteristics of the Gaussian RFIM found by Wu and Machta [28] revealed that the appearance of these strong finite-size effects are independent of the RF distribution and their existence is related to the value of the disorder strength. This observation is not compatible with mean-field theory, since its first-order prediction for only the bimodal case depends on the existence of a minimum at zero-field of the distribution [33]. The present study has illustrated that these characteristics are most likely effects complicating the finite-size behavior of the model but not determining its true asymptotic scaling behavior.

Our results clearly indicate that the interface tension $[\Sigma(L)]_{av}$ vanishes and the two peaks of the energy PDF move together in the thermodynamic limit and therefore provide convincing evidence that the transition is continuous and that there is no TCP along the phase transition line. Consequently, the coexistence between an ordered phase and a disordered phase will be hardly detectable in the thermodynamic limit. Nevertheless, for large but finite systems, the dip represents a considerable barrier between the ordered phase and the disordered one, so that in some sense, one may speak

for a phase coexistence for finite systems. The results of figures 5(a) and 6(a) indicate a linear approach of the interface tension to zero in the limit $L \rightarrow \infty$, and therefore an exponential increase of the ratio P_{max}/P_{min} in L , and point to an unconventional continuous transition, in which the energy PDF will approach two delta functions that move together (see figures 5(b) and 6(b)) in the thermodynamic limit. Such an unconventional behavior has been first predicted by Eichhorn and Binder [77], for the order-parameter PDF of the 3D random-field three-state Potts model. These authors have explained such an unusual behavior by presenting in detail the consequences of a scenario (including leading corrections to scaling) based on a finite-size scaling statement for the order-parameter universal PDF. According to this scenario, the finite-size scaling behavior in RF systems can be recovered and the relative width of the corresponding order-parameter PDF peaks vanishes in the scaling limit as $L^{-\theta/2}$, where θ is the critical exponent describing the violation of hyperscaling ($2 - \alpha = (d - \nu)\theta$). In conclusion, the results of this paper and the observations of references [28, 34, 35] are strong indications of a similar unusual scenario for a continuous transition, calling for further investigation, such as the determination of the exponent θ .

3. Conclusions

Two entropic sampling numerical strategies have been implemented for the study of the first-order-like properties of the 3D bimodal RFIM. Our experience and comparative studies, using different numerical approaches, revealed the sensitivity of the double-peak structure of the energy probability density function of the model, especially with increasing the system size. Thus, the need for careful implementations of entropic sampling techniques in cases of complex systems has been critically discussed. An efficient high-level one-range Wang-Landau approach has been proposed as a quite safe alternative, avoiding subtle problems related to the position and the depth of the minima of the double-peak energy probability density functions.

Reliable data were obtained using this high-level one-range Wang-Landau approach and the corresponding Lee correction for large numbers of random-field realizations and quite large lattice sizes, up to $L = 32$. Using these data and by a systematic finite-size analysis, implementing the Lee-Kosterlitz method, we have studied the nature of the transition at the strong disorder regime. Our results for both the free-energy barrier and latent heat for the ensemble of double-peak random-field realizations suggest a behavior in accordance with a continuous transition. These results disclose the open controversy for the existence of a tricritical point in the phase diagram of the 3D bimodal RFIM at the strong disorder regime and serve in favor of the unusual scenario for a continuous transition, originally proposed by Eichhorn and Binder [77]. It will be interesting to repeat the present investigation for the wide bimodal distribution (with a Gaussian width) and even for the Gaussian distribution, at the strong disorder regime, since this would provide additional confidence to our conclusions.

Acknowledgments

The authors would like to thank Professor A N Berker for useful discussions. Financial support by EPEAEK/PYTHAGORAS under Grant No. 70/3/7357 is gratefully acknowledged. N G Fytas was supported by the Alexander S. Onassis Public Benefit Foundation.

References

- [1] Imry Y and Ma S -K 1975 *Phys. Rev. Lett.* **35** 1399
- [2] Aharony A, Imry Y and Ma S K 1976 *Phys. Rev. Lett.* **37** 1364
- [3] Young A P 1977 *J. Phys. C: Cond. Mat.* **10** L257
- [4] Parisi G and Sourlas N 1979 *Phys. Rev. Lett.* **43** 744
- [5] Grinstein G and Ma S -K 1982 *Phys. Rev. Lett.* **49** 685
- [6] Imbrie J Z 1984 *Phys. Rev. Lett.* **53** 1747
- [7] Villain J 1984 *Phys. Rev. Lett.* **52** 1543
- [8] Schwartz M 1985 *J. Phys. C: Cond. Mat.* **18** 135
Schwartz M and Soffer A 1985 *Phys. Rev. Lett.* **55** 2499
Schwartz M, Gofman M and Nattermann T 1991 *Physica A* **178** 6
- [9] Bray A J and Moore M A 1985 *J. Phys. C: Cond. Mat.* **18** L927
- [10] Houghton A, Khurana A and Seco F J 1985 *Phys. Rev. Lett.* **55** 856
- [11] Young A P and Nauenberg M 1985 *Phys. Rev. Lett.* **54** 2429
- [12] Fisher D S 1986 *Phys. Rev. Lett.* **56** 416
- [13] Binder K and Young A P 1986 *Rev. Mod. Phys.* **58** 801
- [14] Ogielski A T 1986 *Phys. Rev. Lett.* **57** 1251
- [15] Bricmont J and Kupiainen A 1987 *Phys. Rev. Lett.* **59** 1829
- [16] See, e.g the articles by Belanger D P and Nattermann T in *Spin Glasses and Random Fields*, ed A P Young (World Scientific, Singapore, 1998)
- [17] Gofman M, Adler J, Aharony A, Harris A B and Schwartz M 1993 *Phys. Rev. Lett.* **71** 2841
- [18] Cao M S and Machta J 1993 *Phys. Rev. B* **48** 3177
- [19] Falicov A, Berker A N and McKay S R 1995 *Phys. Rev. B* **51** 8266
- [20] Swift M R, Bray A J, Maritan A, Cieplak M and Banavar J R 1997 *Europhys. Lett.* **38** 273
- [21] Anglés d' Auriac J -C and Sourlas N 1997 *Europhys. Lett.* **39**, 473
- [22] Hartmann A K and Nowak U 1999 *Eur. Phys. J. B* **7** 105
- [23] Sourlas N 1999 *Comput. Phys. Commun.* **121** 183
- [24] Machta J, Newman M E J and Chayes L B 2000 *Phys. Rev. E* **62** 8782
- [25] Hartmann A K and Young A P 2001 *Phys. Rev. B* **64** 214419
- [26] Middleton A A and Fisher D S 2002 *Phys. Rev. B* **65** 134411
- [27] Wu Y and Machta J 2005 *Phys. Rev. Lett.* **95** 137208
- [28] Wu Y and Machta J 2006 *Phys. Rev. B* **74** 064418
- [29] Fytas N G and Malakis A 2008 *Eur. Phys. J. B* **61** 111
- [30] Harris A B 1974 *J. Phys. C: Cond. Mat.* **7** 1671
- [31] Berker A N 1984 *Phys. Rev. B* **29** 5243
Berker A N 1993 *Physica A* **194** 72
- [32] Dotsenko V S 2007 *J. Stat. Mech.* P09005
- [33] Aharony A 1978 *Phys. Rev. B* **18** 3318
Aharony A 1978 *Phys. Rev. B* **18** 3328
- [34] Hernández L and Diep H T 1997 *Phys. Rev. B* **55** 14080
- [35] Hernández L and Ceva H *Preprint cond-mat/0702398*
Hernández L and Ceva H *Preprint cond-mat/07092159*

- [36] Mézard M and Young A P 1992 *Europhys. Lett.* **18** 653
Mézard M and Monasson R 1994 *Phys. Rev. B* **50** 7199(R)
- [37] Brézin E and De Dominicis C 1998 *Europhys. Lett.* **44** 13
- [38] Sinova J and Canright G 2001 *Phys. Rev. B* **64** 094402
- [39] Wang F and Landau D P 2001 *Phys. Rev. Lett.* **86** 2050
- [40] Wang F and Landau D P 2001 *Phys. Rev. E* **64** 056101
- [41] Schulz B J, Binder K, Müller M and Landau D P 2003 *Phys. Rev. E* **67** 067102
- [42] Baxter R J and Wu F Y 1973 *Phys. Rev. Lett.* **21** 1294
- [43] Martinos S S, Malakis A and Hadjiagapiou I A 2005 *Physica A* **352** 447
- [44] Schreiber N and Adler J 2005 *J. Phys. A: Math. Gen.* **38** 7253
- [45] Wu F Y 1982 *Rev. Mod. Phys.* **54** 235
- [46] Behringer H and Pleimling M 2006 *Phys. Rev. E* **74** 011108
- [47] Pleimling M and Hüller A 2001 *J. Stat. Phys.* **104** 971
- [48] Binder K 2003 *Physica A* **319** 99
- [49] Martinos S S, Malakis A and Hadjiagapiou I A 2006 *Physica A* **366** 273
- [50] Dayan I, Schwartz M and Young A P 1993 *J. Phys. A: Math. Gen.* **26** 3093
- [51] Aharony A and Harris A B 1996 *Phys. Rev. Lett.* **77** 3700
- [52] Wiseman S and Domany E 1998 *Phys. Rev. Lett.* **81** 22
Wiseman S and Domany E 1998 *Phys. Rev. E* **58** 2938
- [53] Parisi G and Sourlas N 2002 *Phys. Rev. Lett.* **89** 257204
- [54] Malakis A and Fytas N G 2006 *Phys. Rev. E* **73** 016109
Malakis A and Fytas N G 2006 *Eur. Phys. J. B* **51** 257
Fytas N G and Malakis A 2006 *Eur. Phys. J. B* **50** 39
- [55] Lee J and Kosterlitz J M 1990 *Phys. Rev. Lett.* **65** 137
Lee J and Kosterlitz J M 1991 *Phys. Rev. B* **43** 3265
- [56] Dotsenko V I S, Selke W and Talapov A L 1991 *Physica A* **170** 278
- [57] Rieger H and Young A P 1993 *J. Phys. A: Math. Gen.* **26** 5279
- [58] Rieger H 1995 *Phys. Rev. B* **52** 6659
- [59] Newman M E J and Barkema G T 1996 *Phys. Rev. E* **53** 393
- [60] Dukovski I and Machta J 2003 *Phys. Rev. B* **67** 014413
- [61] Lee J 1993 *Phys. Rev. Lett.* **71** 211
- [62] Lee H K, Okabe Y and Landau D P 2006 *Comput. Phys. Commun.* **175** 36
- [63] Yamaguchi C and Okabe Y 2001 *J. Phys. A: Math. Gen.* **34** 8781
- [64] Troyer M, Wessel S and Alet F 2003 *Phys. Rev. Lett.* **90** 120201
- [65] Shell M S, Debenedetti P G and Panagiotopoulos A Z 2002 *Phys. Rev. E* **66** 056703
- [66] Dayal P, Trebst S, Wessel S, Würtz D, Troyer M, Sabhapandit S and Coppersmith S N 2004
Phys. Rev. Lett. **92** 097201
- [67] Adler S, Trebst S, Hartmann A K and Troyer M 2004 *J. Stat. Mech.* P07008
- [68] Zhou C and Bhatt R N 2005 *Phys. Rev. E* **72** 025701(R)
- [69] Poulain P, Calvo F, Antoine R, Broyer M and Dugourd Ph 2006
- [70] Zhou C, Schulthess T C, Torbrügge S and Landau D P 2006 *Phys. Rev. Lett.* **96** 120201
- [71] Belardinelli R E and Pereyra V D 2007 *Phys. Rev. E* **75** 046701
- [72] Malakis A, Peratzakis A and Fytas N G 2004 *Phys. Rev. E* **70** 066128
Malakis A, Martinos S S, Hadjiagapiou I A, Fytas N G and Kalozoumis P 2005 *Phys. Rev. E*
72 066120
- [73] Malakis A, Fytas N G and Kalozoumis P 2007 *Physica A* **383** 351
- [74] Fernández L A, Gordillo-Guerrero A, Martín-Mayor V and Ruiz-Lorenzo J J 2008 *Phys. Rev. Lett.* **100** 057201
- [75] Martín-Mayor V 2007 *Phys. Rev. Lett.* **98** 137207
- [76] Chen S, Ferrenberg A M and Landau D P 1992 *Phys. Rev. Lett.* **69** 1213
Chen S, Ferrenberg A M and Landau D P 1995 *Phys. Rev. E* **52** 1377

- [77] Eichhorn K and Binder K 1996 *J. Phys. C: Cond. Mat.* **8** 5209